

Process of energy conservation in the extremely haloalkaliphilic methyl-reducing methanogen *Methanonatronarchaeum thermophilum*

Steiniger, Fabian; Sorokin, Dimitry Y.; Deppenmeier, Uwe

DOI

[10.1111/febs.16165](https://doi.org/10.1111/febs.16165)

Publication date

2021

Document Version

Final published version

Published in

FEBS Journal

Citation (APA)

Steiniger, F., Sorokin, D. Y., & Deppenmeier, U. (2021). Process of energy conservation in the extremely haloalkaliphilic methyl-reducing methanogen *Methanonatronarchaeum thermophilum*. *FEBS Journal*, 289(2), 549-563. <https://doi.org/10.1111/febs.16165>

Important note

To cite this publication, please use the final published version (if applicable). Please check the document version above.


Copyright

Other than for strictly personal use, it is not permitted to download, forward or distribute the text or part of it, without the consent of the author(s) and/or copyright holder(s), unless the work is under an open content license such as Creative Commons.

Takedown policy

Please contact us and provide details if you believe this document breaches copyrights. We will remove access to the work immediately and investigate your claim.

Process of energy conservation in the extremely haloalkaliphilic methyl-reducing methanogen *Methanonatronarchaeum thermophilum*

Fabian Steiniger¹, Dimitry Y. Sorokin^{2,3} and Uwe Deppenmeier¹ 

¹ Institute of Microbiology and Biotechnology, University of Bonn, Bonn, Germany

² Research Centre of Biotechnology, Winogradsky Institute of Microbiology, Russian Academy of Sciences, Moscow, Russia

³ Department of Biotechnology, Delft University of Technology, Delft, The Netherlands

Keywords

climate change; methane; methanogenesis; phenazine; respiratory chain

Correspondence

U. Deppenmeier, Institute of Microbiology and Biotechnology, University of Bonn, Meckenheimer Allee 168, 53115 Bonn, Germany

Tel: +49 228 735590

E-mail: udeppen@uni-bonn.de

Website: <http://www.ifmb.uni-bonn.de/forschung/math.-nat.-fakultaet/ag-prof.-deppenmeier>

(Received 28 June 2021, revised 5 August 2021, accepted 24 August 2021)

doi:10.1111/febs.16165

The recently isolated methanogen *Methanonatronarchaeum thermophilum* is an extremely haloalkaliphilic and moderately thermophilic archaeon and belongs to the novel class Methanonatronarchaeia in the phylum Halobacteriota. The knowledge about the physiology and biochemistry of members of the class Methanonatronarchaeia is still limited. It is known that *M. thermophilum* performs hydrogen or formate-dependent methyl-reducing methanogenesis. Here, we show that the organism was able to grow on all tested C₁-methylated substrates (methanol, trimethylamine, dimethylamine, monomethylamine) in combination with formate or molecular hydrogen. A temporary accumulation of intermediates (dimethylamine or/and monomethylamine) in the medium occurred during the consumption of trimethylamine or dimethylamine. The energy conservation of *M. thermophilum* was dependent on a respiratory chain consisting of a hydrogenase (VhoGAC), a formate dehydrogenase (FdhGHI), and a heterodisulfide reductase (HdrDE) that were well adapted to the harsh physicochemical conditions in the natural habitat. The experiments revealed the presence of two variants of energy-conserving oxidoreductase systems in the membrane. These included the H₂: heterodisulfide oxidoreductase system, which has already been described in *Methanosarcina* species, as well as the novel formate: heterodisulfide oxidoreductase system. The latter electron transport chain, which was experimentally proven for the first time, distinguishes the organism from all other known methanogenic archaea and represents a unique feature of the class Methanonatronarchaeia. Experiments with 2-hydroxyphenazine and the inhibitor diphenyleneiodonium chloride indicated that a methanophenazine-like cofactor might function as an electron carrier between the hydrogenase/formate dehydrogenase and the heterodisulfide reductase.

Abbreviations

CoM-S-S-CoB, heterodisulfide of HS-CoM and HS-CoB; DMA, dimethylamine; DPI, diphenyleneiodonium chloride; Fd, ferredoxin; Fdh, membrane-bound formate dehydrogenase; Fd_{ox}, oxidized ferredoxin; Fd_{red}, reduced ferredoxin; FeS, iron-sulfur; Hdr, heterodisulfide reductase; HS-CoB, 7-mercaptoheptanoylthreonine phosphate; HS-CoM, 2-mercaptoethanesulfonate; M., *Methanonatronarchaeum*; MMA, monomethylamine; MPhen, methanophenazine; MPhen_{red}, reduced methanophenazine; MV, methyl viologen; OD₆₀₀, optical density at 600 nm; OD_{max}, final optical density; OH-Phen, 2-hydroxyphenazine; t_d, doubling time; TMA, trimethylamine; Vho, membrane-bound hydrogenase.

Introduction

Methanogenic archaea play a crucial role in the carbon cycle. They metabolize the end products of the anaerobic decomposition of organic material by hydrolytic and fermenting bacteria to methane, a powerful climate gas [1–4]. A variety of new methanogenic genera and species have been isolated from extreme ecosystems such as hypersaline or extremely cold habitats [5,6]. The study of the influence of these ecosystems on global climate and investigation of the organisms involved is of great interest. Among the newly discovered organisms are two genera of extremely (halo)alkaliphilic methyl-reducing methanogens forming the new class of *Methanonatronarchaeia* [7,8]. These organisms are only distantly related to the taxonomic groups of methanogenic archaea currently described and, according to the recent phylogenomic-based analysis, represent a deep phylogenetic lineage branching at the base of a new phylum ‘Halobacteriota’ [9,10].

Methanogenic archaea differ with respect to their substrate spectrum and the pathway of methanogenesis. The hydrogenotrophic methanogens use carbon dioxide and H₂ or formate as substrates to form methane [11], and the acetoclastic microorganisms metabolize acetate to carbon dioxide and methane [4,12]. The third group are the methylotrophic methanogens, which convert methylated compounds such as methanol, methylamines, and methyl sulfides to methane [13,14]. Moreover, methanogens were discovered, which use methoxylated aromatic compounds as source for methyl groups [15]. In this pathway, part of the methyl groups are oxidized to CO₂ and the resulting reducing equivalents are used for the reduction in the remaining methyl groups to methane. In addition, some methanogens have been described that cannot oxidize the methyl groups. Instead, they reduce methylated compounds to methane using electrons derived from the oxidation of hydrogen [16–19]. This variation of methylotrophic methanogenesis is referred to as methyl reduction.

Methanonatronarchaeum thermophilum AMET1^T (*M. thermophilum*; DSM 28684) belongs to the aforementioned new class of *Methanonatronarchaeia* and is an extremely haloalkaliphilic and moderately thermophilic methanogen living in sulfidic sediments of hypersaline soda lakes [7]. The organism is able to reduce methanol and methylamines to methane using H₂ as a reductant [8]. In contrast to all other methanogens that rely on H₂-dependent reduction in methylated C₁-compounds, this organism is also able to use formate as an electron donor for this process of methanogenesis.

Sorokin *et al.* [7] postulated a corresponding metabolic model based on growth experiments and bioinformatic analyses. According to this model, the oxidation of formate is catalyzed by a membrane-bound formate dehydrogenase (FdhGHI), whereas the oxidation of H₂ takes place via a membrane-bound hydrogenase (VhoGAC). Based on this, the electrons fed into the anaerobic respiratory chain by FdhGHI and VhoGAC are subsequently used by a membrane-bound heterodisulfide reductase (HdrDE) to reduce the heterodisulfide (CoM-S-S-CoB), which is the terminal electron acceptor of this system. So far, three energy-conserving, membrane-bound electron transport systems are known in methanogens: (a) H₂: CoM-S-S-CoB oxidoreductase, (b) coenzyme F₄₂₀H₂: CoM-S-S-CoB oxidoreductase, and (c) reduced ferredoxin: CoM-S-S-CoB oxidoreductase [12]. The formate-dependent electron transport system would be a new feature that could be used for the generation of an electrochemical ion gradient across the cytoplasmic membrane. The utilization of formate for methanogenesis was previously only known from some hydrogenotrophic methanogens, which use formate as a source of electrons to reduce CO₂ to methane [1,11].

Here, we present experimental data describing the electron flow in membranes of the type strain *M. thermophilum* AMET1^T from the class *Methanonatronarchaeia*. Based on membrane preparations, we provide biochemical proof that electron flow occurs from formate or hydrogen to CoM-S-S-CoB. Furthermore, we provide first evidence that a methanophenazine (MPhen) derivative is the potential electron carrier in the membranes of *M. thermophilum* AMET1^T.

Results

Growth parameters

The knowledge about the physiology and biochemistry of members of the class *Methanonatronarchaeia* and the enzymes, which are involved in the methanogenic pathway, is still limited. Recently, multiple strains of *M. thermophilum* were enriched and further isolated in pure culture using a combination of C₁-methylated compounds as electron acceptors in combination with formate or hydrogen as the external electron donors [7,8]. Here, we present detailed growth data showing that *M. thermophilum* AMET1^T was able to grow on all tested substrates (methanol, trimethylamine (TMA), dimethylamine (DMA), monomethylamine (MMA)) in combination with formate or molecular hydrogen. However, different doubling times and final optical densities (OD_{max}) were observed, although equimolar

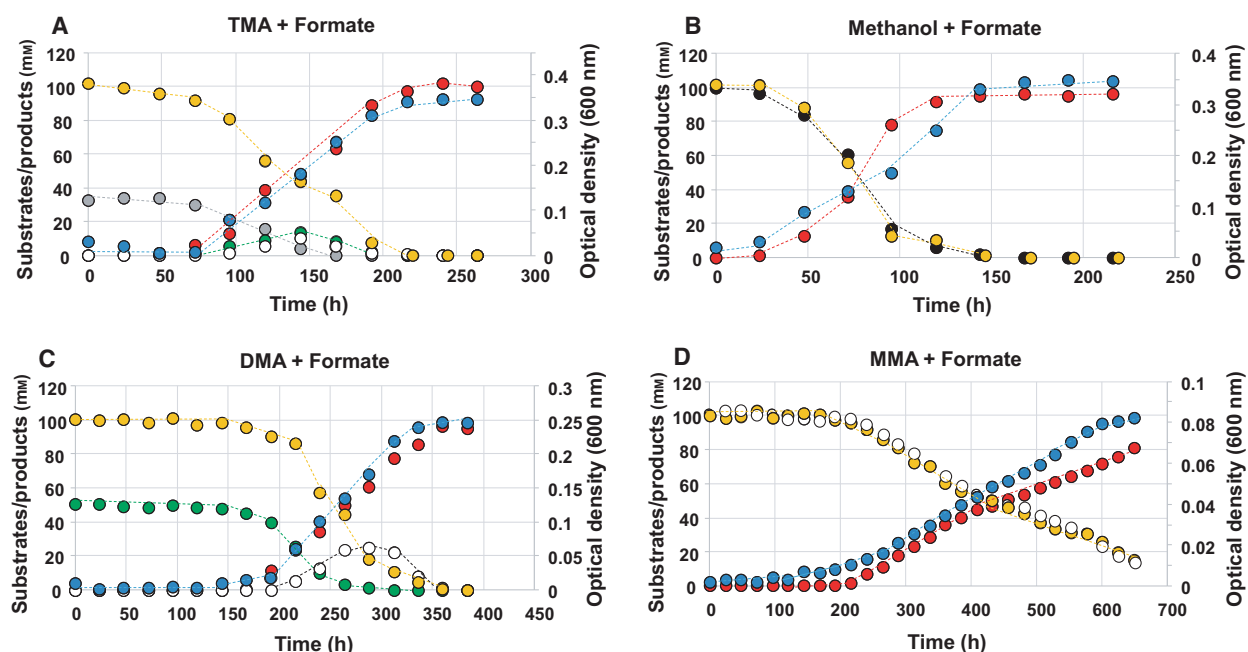


Fig. 1. Growth parameter of *M. thermophilum* during methanogenesis from methylated C₁-compounds and formate. (A) 33.3 mM TMA, (B) 100 mM methanol, (C) 50 mM DMA, (D) 100 mM MMA. Experiments were performed in 50-mL serum flasks under an atmosphere of N₂/CO₂ (80%/ 20%) with 100 mM formate as described in Materials and Methods. Yellow circles: formate; black circles: methanol; red circles, methane; gray circles: TMA; green circles: DMA; white circles: MMA; blue circles: optical density (OD₆₀₀). The experiments were performed three times. One representative experiment is shown for each substrate combination.

amounts of available methyl groups were added (methanol 100 mM, TMA 33.3 mM, DMA 50 mM, and MMA 100 mM). The organism showed the fastest growth ($t_d = 44.3 \pm 2.0$ h) using the substrates TMA and formate (Fig. 1A). Similar t_d values were obtained for methanol with formate (48.8 ± 1.0 h) and DMA with formate (49.7 ± 1.3 h; Fig. 1B,C). The doubling time with MMA as a substrate in combination with formate was distinctly longer, with 75.1 ± 5.2 h (Fig. 1D). OD_{max} values for methanol and TMA with formate were in the range of 0.35. In the case of DMA and MMA, the values were comparatively lower (OD_{max} = 0.25 and 0.08, respectively). In general, it was observed that the consumption of formate and methyl groups and methane formation took place in a 1 : 1 : 1 stoichiometry. The methyl groups applied were completely reduced to methane with the help of formate. TMA contains three methyl groups, which are sequentially transferred to HS-CoM in the course of methane formation. Hence, there are two possible intermediates, DMA and MMA. Similarly, DMA contains two methyl groups and MMA could be an intermediate. Therefore, the question arose of whether these intermediates were accumulated or whether TMA and DMA were immediately converted to CH₄

and NH₃. In cultures grown on TMA plus formate, significant amounts of DMA appeared in the culture supernatant with the highest concentration of 11 mM after 144 h. In addition, MMA was secreted in the medium, with the highest concentration of 10 mM after 144 h. Both, DMA and MMA, concentrations decreased in the further cultivation process and were completely consumed at the end of the growth experiments. In the cultures grown on DMA with formate, an increase in the MMA concentration in the medium was observed. After 288 h, approx. 25 mM MMA was detected. However, in the course of cultivation, MMA in the medium was also completely consumed. Interestingly, the temporary accumulation of intermediates (DMA or/and MMA) in the medium occurring during the metabolism of TMA or DMA has already been described for *Methanomassiliicoccus luminyensis* and *Methanosarcina mazei* [20,21]. Furthermore, the results are consistent with the presence of the genes in the genome of *M. thermophilum* AMET1^T, which encode all necessary methyltransferases (Fig. 2A) for the utilization of methylamines and methanol (Fig. 2B) [7].

In comparison with hydrogen instead of formate as a reducing agent (Fig. 3), similar doubling times of 45.4 ± 2.0 h (methanol; Fig. 3A), 46.7 ± 2.0 h (TMA;

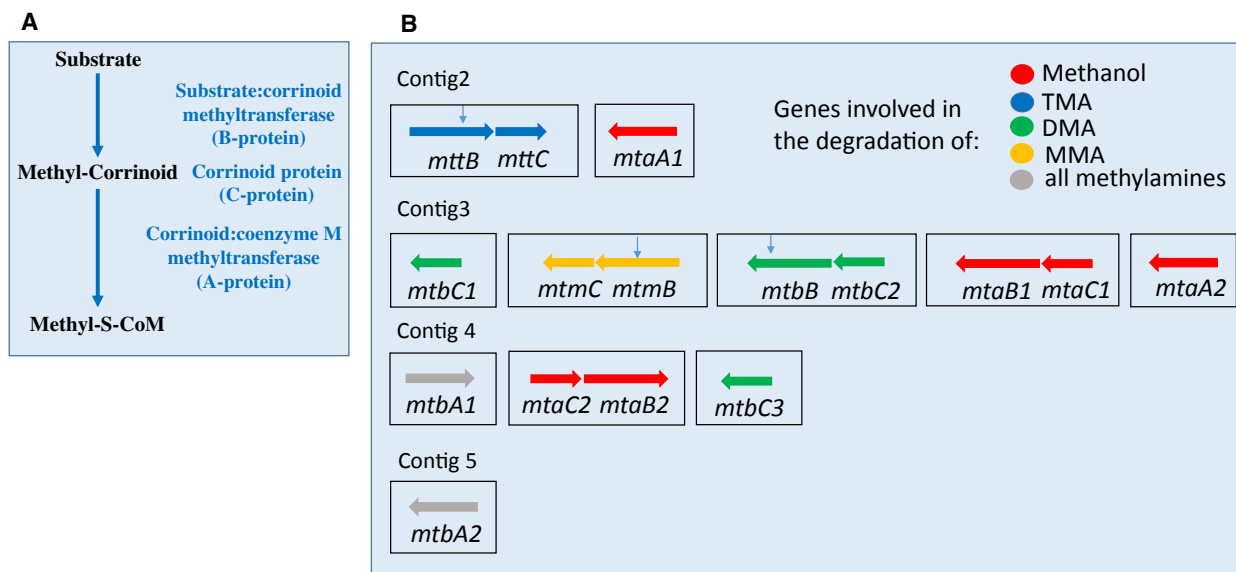


Fig. 2. Methyl group transfer from methylated substrates in *M. thermophilum*. (A) General scheme. Substrate: corrinoid methyltransferases (B-protein) forward methyl groups from the substrate to a corrinoid-containing methyl-accepting protein (C-protein). From the methylated corrinoid proteins, the methyl moieties are transferred to HS-CoM as catalyzed by corrinoid: coenzyme M methyltransferases (A-protein). (B) Localization of genes according to Ref. [7]. B and C-proteins are substrate specific and are encoded by the genes *mtaB/C* for methanol, *mttB/C* for TMA, *mtbB/C* for DMA, and *mtmB/C* for MMA utilization. There are two types of A-proteins, MtaA and MtbA, which use MtaC and MttC, MtbC or MtmC for methylation of HS-CoM, respectively. Contig 2—*mttB*: OIJ19433.1/OIJ19434.1; *mttC*: WP_086636534.1; *mtaA1*: WP_086636593.1. Contig 3—*mtbC1*: WP_086636757.1; *mtmB*: OIJ18809.1/ OIJ18808.1; *mtmC*: WP_086636534.1; *mtbB*: OIJ19071.1/ OIJ19070.1; *mtbC2*: WP_086637115.1; *mtaB1*: WP_086637136.1; *mtaC1*:WP_086637137.1; *mtaA2*: WP_086637345.1. Contig 4: *mtbA1*: WP_161490776.1; *mtaC2*: WP_086637445.1; *mtaB2*: WP_086637136.1, *mtbC3*: WP_086637468.1. Contig 5: *mtbA2*: WP_143406904.1. Methyltransferases (B-proteins) initiating methanogenesis from TMA, DMA, and MMA possess a novel residue, pyrrolysine, which is encoded by a single amber(UAG) codon (blue arrow).

Fig. 3B), 49.0 ± 1.2 h (DMA; Fig. 3C), and 94.3 ± 1.0 h (MMA; Fig. 3D) were obtained. The consumption of the methyl groups and the release of methane also occurred in equimolar ratios. For growth on TMA and DMA, the data likewise showed that the intermediates DMA and MMA were released into the medium to a similar extent as in the cultures with formate and were subsequently completely consumed. Interestingly, the growth yields were significantly lower than in the cultures with formate, with OD_{max} values of 0.23 (methanol and TMA), 0.125 (DMA), and 0.05 (MMA).

Analysis of enzymes involved in the respiratory chain of *M. thermophilum*

The growth analysis shown above and the data of Sorokin *et al.* [7] and Borrel *et al.* [22] led to the hypothesis that the energy conservation of *M. thermophilum* is dependent on a respiratory chain consisting of a hydrogenase, a formate dehydrogenase, and a heterodisulfide reductase. It is predicted that the H_2 -dependent membrane-bound electron transport is catalyzed by the

hydrogenase VhoGAC and the heterodisulfide reductase HdrDE, which reduces CoM-S-S-CoB. If formate serves as the electron donor, it is most likely that the membrane-bound formate dehydrogenase FdhGHI oxidizes the electron donor, and the electrons are then transported via an unknown electron carrier in the membrane to the heterodisulfide reductase, which reduces the final electron acceptor CoM-S-S-CoB to coenzyme M and coenzyme B.

To prove the presence of the three key enzyme complexes in *M. thermophilum* biochemically, we tested the activity of membrane preparations with respect to the oxidation of formate and H_2 and the reduction of heterodisulfide using the artificial electron carrier methyl viologen (MV, Table 1). We detected a total Vho activity of 20.0 ± 0.3 U mg membrane protein⁻¹.

To measure FdhGHI activity, the gas atmosphere was N_2 , formate served as electron donor, and MV was added as an electron acceptor. In membrane fractions of *M. thermophilum*, an FdhGHI activity of 5.9 ± 0.1 U mg protein⁻¹ was observed. To examine the activity of the HdrDE complex in the membrane, the natural electron acceptor CoM-S-S-CoB was

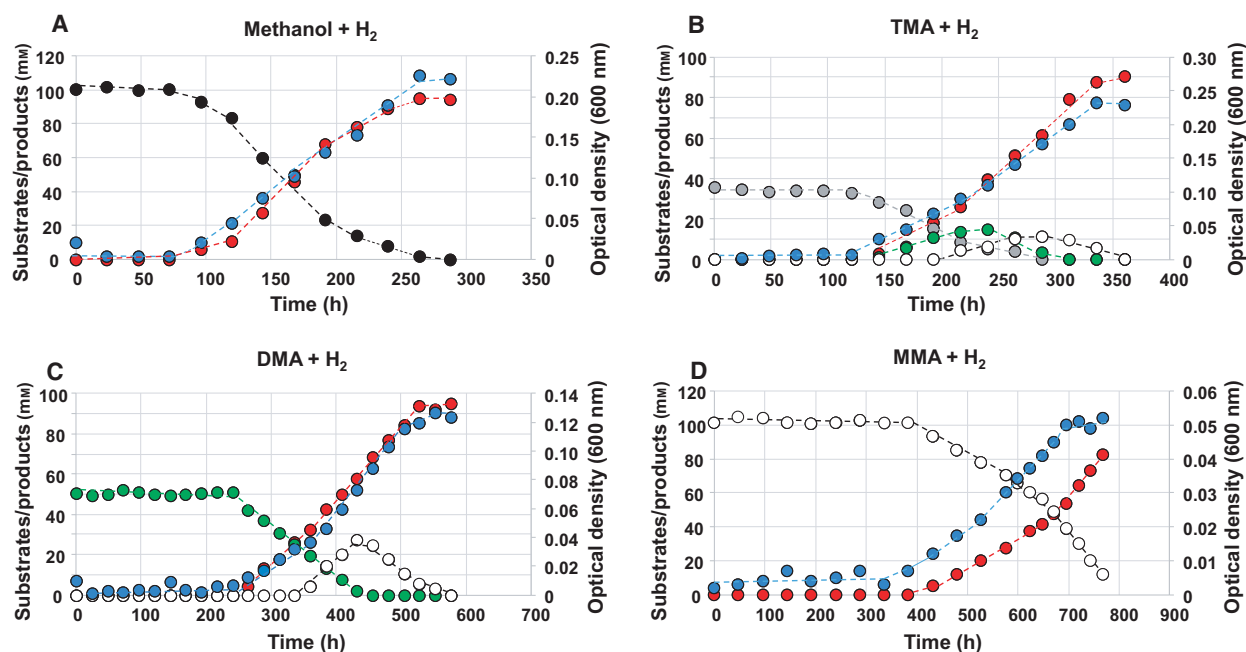


Fig. 3. Growth parameters of *M. thermophilum* grown on methanol and methylamines with H_2 as reducing agent. (A) 100 mM methanol. (B) 33.3 mM TMA. (C) 50 mM DMA. (D) 100 mM MMA. Experiments were performed in 50-mL serum flasks under an atmosphere of H_2 as described in Materials and Methods. Black circles: methanol; red circles, methane; gray circles: TMA; green circles: DMA; white circles: MMA; blue circles: optical density (OD_{600}). The experiments were performed three times. One representative experiment is shown for each substrate combination.

Table 1. Specific activities of enzymes involved in membrane-bound electron transfer.

	Electron donor	Electron acceptor	DPI ^a	Specific activity ^{b,c} (U·mg ⁻¹ membrane protein)
FdhGHI	Formate	MV	–	5.9 ± 0.1
FdhGHI	Formate	MV	+	5.9 ± 0.2
VhoGAC	H_2	MV	–	20.0 ± 0.3
VhoGAC	H_2	MV	+	20.2 ± 0.3
HdrDE	MV_{red}	CoM-S-S-CoB	–	3.3 ± 0.2
HdrDE	MV_{red}	CoM-S-S-CoB	+	3.4 ± 0.2

^a1 $\mu\text{mol} \cdot \text{mg}$ membrane protein⁻¹ diphenyleneiodonium chloride (DPI) was added as indicated.; ^bAssay conditions for FdhGHI and VhoGAC: pH 9.5, 2 M NaCl; assay conditions for Hdr: pH 8.5, 2 M KCl.; ^cThe experiments were performed three times.

added. Reduced methyl viologen (MV_{red}) was used as an artificial electron donor. The specific activity for CoM-S-S-CoB reduction in the membrane preparations was 3.3 ± 0.2 U mg protein⁻¹ (Tab. 1). These results strongly indicated that all expected enzymes are catalytically active in the membrane compartment of *M. thermophilum*.

For a detailed analysis of the individual enzymes and to get an impression of their adaptation to the

natural habitat of *M. thermophilum*, we analyzed the enzymes with regard to their dependence on pH (Fig. 4A–C) and ions (Fig. 4D–F). The organism was isolated from a hypersaline soda lake and is an obligate haloalkaliphilic methanogen, with an optimum growth at pH 9.5–9.8 and 4 M total Na^+ [7]. The catalytic subunits of the hydrogenase (VhoA) and the formate dehydrogenase (FdhH) are most likely oriented toward the extracellular space [23–25] and thus exposed to the conditions in the natural habitat. In contrast, the catalytic subunit of heterodisulfide reductase (HdrD) is located at the cytoplasmic side of the cytoplasmic membrane. In addition, the organism accumulates about 2.2 M KCl in the cytoplasm due to its most probable ‘salt-in’ osmoprotection strategy [7,8]. Therefore, analysis of the pH optimum was performed at a salinity of 2 M NaCl and 2 M KCl, respectively. The highest hydrogenase activity (31.2 ± 8.3 U mg protein⁻¹) was detected at a pH value of 9.5 and 2 M NaCl (Fig. 4B). The activity was about 20% lower when KCl was used instead of NaCl in the buffer. The analysis of the optimal ion concentration was therefore carried out with NaCl at a pH of 9.5. The highest activity of 46.9 ± 7.4 U mg protein⁻¹ was obtained with 1 M NaCl (Fig. 4E). However, even with 0 M and 2 M NaCl, more than 63% of the

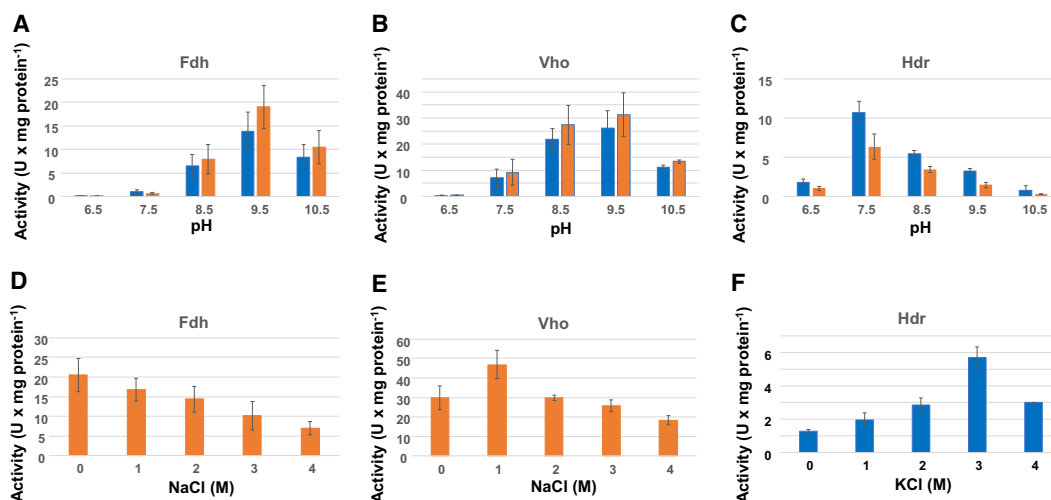


Fig. 4. Adaptation of Vho, Fdh, and Hdr from *M. thermophilum* toward pH and salinity. Analysis was performed with the artificial electron carrier MV in rubber-stoppered anaerobic glass vials (material and methods). For hydrogenase activity determination, the gas atmosphere was molecular hydrogen, whereas Fdh and Hdr activity was measured under a nitrogen atmosphere. (A) FdhGHI activity; (B) VhoGAC activity; (C) HdrDE activity. Orange bars, assays with 2 M NaCl; blue bars, assays with 2 M KCl. (D) FdhGHI activity (pH 9.5); (E) VhoGAC activity (pH 9.5); (F) HdrDE activity (pH 8.5). The values represent the average of three different experiments using different membrane preparations. Standard deviations are indicated by error bars.

maximum activity was still present. Using 4 M NaCl, 40% of the maximum activity was observed. FdhGHI showed the highest specific activity at a pH of 9.5 in the presence of 2 M NaCl (Fig. 4A). Formate oxidation was slightly lower with 2 M KCl instead of NaCl. Therefore, the activity tests were carried out with NaCl at a pH value of 9.5. Interestingly, the specific activity was highest in the absence of NaCl (20.5 ± 4.2 U mg protein⁻¹) and decreased with increasing ion concentration (Fig. 4D). However, it should be noted that even at a NaCl concentration of 4 M, 34% of the maximum activity was still present. In summary, the enzymes were well adapted to the natural physico-chemical conditions and showed adaptation to a wide range of ion concentrations.

HdrDE showed its highest activity at a pH value of 7.5 with 10.7 ± 1.4 U · mg protein⁻¹ in the presence of 2 M KCl (Fig. 4C). Even at a pH of 8.5, about 50% of the activity was still present. The enzyme activity was higher with potassium chloride than with sodium chloride. At pH 7.5, the specific activity with 2 M potassium chloride was about 40% higher than with 2 M sodium chloride. Therefore, the analysis of the salt dependence was carried out with potassium chloride at a pH of 8.5 (Fig. 4F). The highest activity was obtained with 3 M KCl (3.8 ± 0.4 U mg protein⁻¹). With 2 and 4 M KCl, about 50% of the activity was still present. The higher activities with KCl compared with NaCl probably represent an adaptation to the concentration of 2.2 M KCl in the cells and is an

additional confirmation of the proposed haloarchaeal type of osmoprotection in *Methanonatronarchaeum* [7].

Analysis of H₂: CoM-S-S-CoB and formate: CoM-S-S-CoB oxidoreductase

To analyze the electron transfer between the enzymes described above, the entire membrane-bound electron transport from H₂ or formate to CoM-S-S-CoB was analyzed (Fig. 5). The H₂: CoM-S-S-CoB oxidoreductase system, already described in other species such as *Methanosarcina mazei* [12], was measured under an H₂ atmosphere after adding CoM-S-S-CoB as electron acceptor. Thiol formation proceeded with a velocity of 784 ± 51.4 nmol mg⁻¹ · min⁻¹ in the presence of H₂. Hence, 392 ± 25.7 nmol CoM-S-S-CoB was reduced per min and mg membrane protein. The reaction only took place whether membranes, CoM-S-S-CoB, and molecular hydrogen were present (Fig. 5).

Thiol production from the reduction in CoM-S-S-CoB with formate as electron donor was also measured with a rate of 369 ± 35 nmol mg⁻¹ · min⁻¹ under an N₂ atmosphere (Fig. 5). Therefore, 184.5 ± 17.5 nmol CoM-S-S-CoB was reduced per min and mg membrane protein. The formation of thiols was only observed in the complete assay with membranes, CoM-S-S-CoB, and formate. The results confirmed the presence of the novel formate: CoM-S-S-CoB oxidoreductase system in the membranes of *M. thermophilum*. This system, which has been experimentally proven for

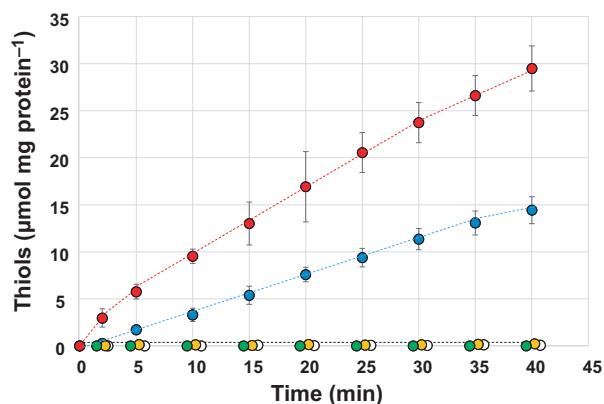


Fig. 5. Electron transport from H₂ or formate to CoM-S-S-CoB in *M. thermophilum*. The complete assay contained 200 µL 100 mM Tris/HCl buffer (pH 8.5, 2 M NaCl), 5 mM CoM-S-S-CoB, and 50 µg membrane protein. Blue circles: Complete assay with 10 mM formate, membranes, and CoM-S-S-CoB. Red circles: Complete assay with H₂, membranes, and CoM-S-S-CoB. Green circles: Formate and H₂ omitted. White circles: Membranes omitted. Yellow circles: CoM-S-S-CoB omitted. The values represent the average of three different experiments using different membrane preparations. Standard deviations are indicated by error bars.

the first time, distinguishes the organism from all other known methanogenic archaea and represents a unique feature of the class Methanonatronarchaea.

We also tested diphenyleioidonium chloride (DPI) for its effect on membrane-bound electron transport. DPI is a potential inhibitor of flavoproteins and low potential cytochromes (Fig. 6) [26,27]. DPI is also an analogue of methanophenazine and blocks electron flow in membranes of *Methanosarcina mazei* [28]. The electron transport within the H₂: CoM-S-S-CoB and formate: CoM-S-S-CoB oxidoreductase of *M. thermophilum* was also inhibited by DPI (Fig. 6). With 0.1 µmol DPI per mg membrane protein, the thiol formation rate decreased by 45% (formate) and 33% (H₂) compared to the activity without DPI. In the presence of 1.0 µmol DPI mg protein⁻¹, the residual activity was only 14% and 12%, respectively. In contrast to the overall electron transport, the activity of the FdhGHI and VhoGAC with MV as electron acceptor was not inhibited by DPI. This was also true for electron transfer from MV_{red} to CoM-S-S-CoB as catalyzed by HdrDE (Tab. 1). This effect is due to the process of electron transport within the enzyme complexes and is explained in detail in the Discussion.

To further verify that a MPhen derivative is the potential soluble electron carrier in the membranes of *M. thermophilum*, we performed additional photometric

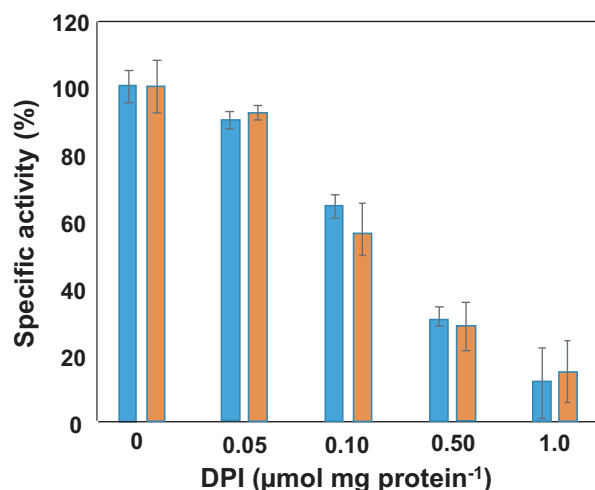


Fig. 6. Influence of DPI on electron flow in the respiratory chain of *M. thermophilum*. Reaction assays contained 200 µL 100 mM Tris/HCl buffer (pH 8.5, 2 M NaCl), 5 mM heterodisulfide, and 50 µg membrane protein. After the addition of DPI (as indicated) and incubation for 5 min, the reaction was started by gassing with H₂ or by the addition of 10 mM formate. 100% activity corresponded to 360 ± 17 nmol and 269 ± 21 nmol CoM-S-S-CoB reduction per min and per mg membrane protein with H₂ and formate as electron donor, respectively. The experiment was conducted in triplicate using different membrane preparations. Standard deviations are indicated by error bars. Blue bars, H₂ + CoM-S-S-CoB. Orange bars, formate + CoM-S-S-CoB.

enzyme assays with the MPhen analogue 2-hydroxyphenazine (OH-Phen). The compound is reasonably soluble in water and is an excellent analogue to MPhen in enzymatic assays [28]. The electron transfer from formate or hydrogen to OH-Phen in the presence of membranes of *M. thermophilum* proceeded with a rate of 1.4 ± 0.6 U mg protein⁻¹ (formate) and 9.6 ± 2.0 U mg protein⁻¹ (H₂), respectively (Fig. 7A/B). After complete consumption of formate, reduced OH-Phen was almost completely reoxidized upon the addition of heterodisulfide with a specific activity of 0.6 ± 0.2 U mg protein⁻¹ (Fig. 7B). As shown above for the entire electron transport chain, DPI also inhibited the reaction of the single enzymes with OH-Phen (not shown).

Discussion

In addition to the triple extreme growth conditions (high salt, high pH, moderately high temperature), members of the new class Methanonatronarchaea show some further special features. For example, the genes for the oxidative branch of methanogenesis are incomplete. Thus, the membrane-bound methyltransferase (Mtr) and the formyl-methanofuran dehydrogenase

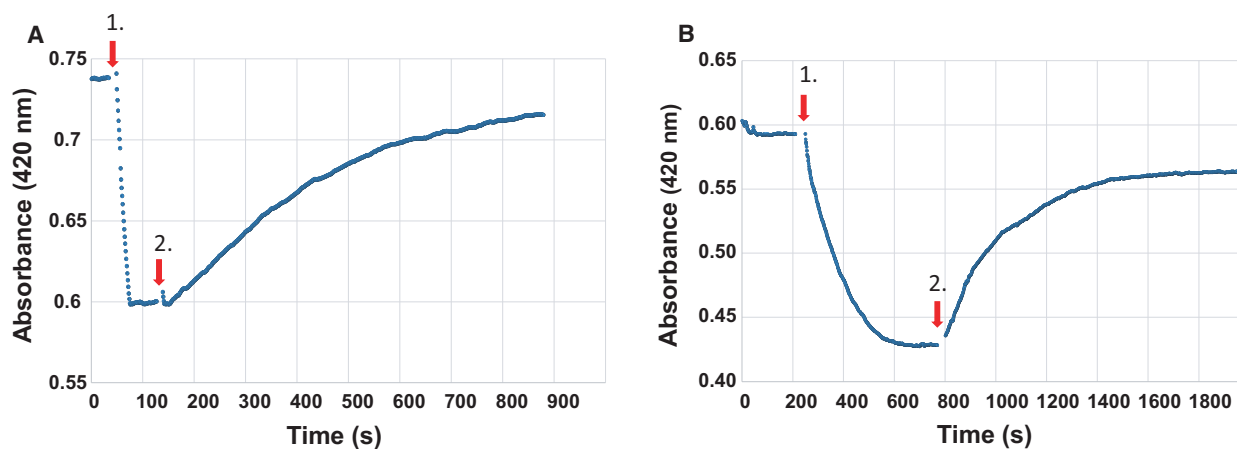


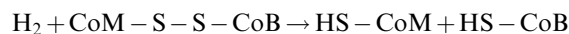
Fig. 7. Membrane-bound electron transport in *M. thermophilum* with OH-Phen. (A) Reduction in OH-Phen by VhoGAC in the presence of H_2 and reoxidation by HdrDE. (B) Reduction in OH-Phen by FdhGHI in the presence of formate and reoxidation by HdrDE. The complete assay contained 700 μ L 100 mM Tris/HCl buffer (pH 8.5, 2 M NaCl, 5 mM dithiothreitol, 1 μ g/mL resazurin), 200 μ M OH-Phen, and 7.5 μ g membrane protein. Detailed assay conditions are described in Materials and Methods. Arrow 1: Addition of 50 μ M formate or H_2 . Arrow 2: Addition of CoM-S-CoB. The experiment was conducted in triplicate using different membrane preparations. One representative experiment is shown.

(Ftr) are missing. The soluble heterodisulfide reductase HdrABC is also absent [7]. Hence, there are some major differences to the previously known methanogenic archaea, and the investigation of the energy metabolism is of special interest. Based on this, we performed experiments to elucidate the mechanisms of ATP synthesis of *M. thermophilum* AMET1^T, the type strain of the genus *Methanonatronarchaeum*.

Methanogenic archaea can be divided into two major groups based on their energy conservation. Members of the order Methanosarcinales possess a membrane-bound respiratory chain, with cytochromes, MPhen, and several membrane-bound enzymes, which translocate ions (H^+ or Na^+) across the cytoplasmic membrane and generate an electrochemical ion gradient ($\Delta\mu_{H^+}$ and $\Delta\mu_{Na^+}$) [3,12]. In contrast, obligate CO_2 -reducing methanogens lack cytochromes and membrane-bound electron transport chains [13,29]. In these methanogenic archaea, only the membrane-bound methyltransferase is directly involved in the formation of a $\Delta\mu_{Na^+}$ [29]. Fd_{red} , necessary for the endergonic reduction in CO_2 , is provided by an electron bifurcating reaction of a soluble heterodisulfide reductase (HdrABC) and a cytoplasmic hydrogenase (MvhAGD) [30]. Another group of methanogens forms methane from the H_2 -dependent reduction in methylated C_1 -compounds [15]. One example is *Methanosphaera stadtmanae* [17], which uses the HdrABC/MvhAGD complex for Fd_{red} production. Fd_{red} is then reoxidized by the multisubunit hydrogenase Ehb in the membrane, forming H_2 and an electrochemical ion gradient [13]. Hence, the mode of energy

conservation in *Methanosphaera stadtmanae* resembles the one in obligate CO_2 -reducing methanogens. In principle, also *M. thermophilum* performs an H_2 -dependent reduction in methylated C_1 substrates for methanogenesis; however, the processes for the formation of an electrochemical ion gradient are totally different compared with *Methanosphaera stadtmanae*. The biochemical data presented here showed that *M. thermophilum* contains an active membrane-bound hydrogenase (VhoGAC) and an active heterodisulfide reductase (HdrDE) (Figs 8 and 9A/B), which are highly homologous to the corresponding enzymes from *Methanosarcina* species. In addition to VhoGAC, *M. thermophilum* contains genes encoding a membrane-bound multisubunit hydrogenase complex, which is distantly related to NADH dehydrogenases. In contrast to VhoGAC, this hydrogenase possibly provides Fd_{red} for anabolism [15].

In *Methanosarcina mazei* and *Methanosarcina barkeri*, VhoGAC and HdrDE constitute an electron transport system that is referred to as H_2 : heterodisulfide oxidoreductase (Eqn 1).



$$(\Delta G^0 = -51.9 \text{ kJ} \cdot \text{mol}^{-1}) \quad (1)$$

The hydrogenase consists of the subunits VhoGA and contains several FeS centers and the Ni/Fe center, which is responsible for H_2 oxidation. The membrane-integral subunit VhoC contains heme b and transfers electrons to the natural electron carrier MPhen (Figs 8

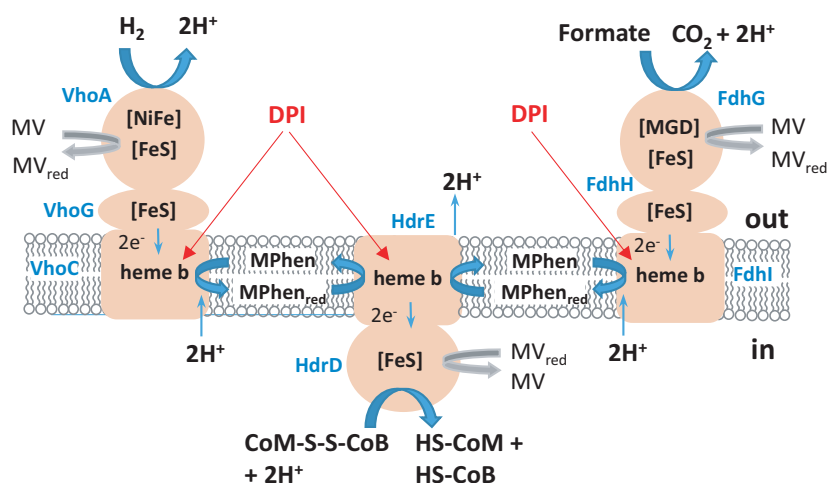
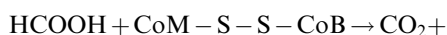


Fig. 8. Tentative membrane-bound electron transport chain in *M. thermophilum*. Blue arrows show the pathway of electron transport within the respiratory chain. Red arrows indicated the inhibition of heme b groups by DPI. Grey arrows represent the sites of MV reduction and MV_{red} oxidation. The subunits of the complexes are indicated in blue. Based on the postulated reaction mechanisms of the enzymes, it is concluded that an electrochemical proton gradient is established. However, the H⁺ gradient could be converted to a Na⁺ gradient with the help of a Na⁺/H⁺-antiporter. MGD, molybdopterin-guanine dinucleotide. FeS, iron-sulfur cluster. NiFe, nickel-iron cluster. Protein numbers: VhoGAC, WP_086636999 - WP_086637001; FdhGHI, WP_201721220.1, WP_086636543.1, WP_086636545.1; HdrDE, WP_086637509—WP_086637510.

and 9 A). In the course of the reaction, two protons are translocated across the cytoplasmic membrane [12,31]. Genetic and biochemical data support the assumption that VhoA is cotranslocated with VhoG across the cytoplasmic membrane [23]. Therefore, it is most likely that the active center of the enzyme is located at the periplasmic side of the membrane [24,32]. The heterodisulfide reductase catalyzes the final step in the anaerobic respiratory chain of *Methanosarcina* species. The HdrDE enzyme is firmly integrated into the membrane by the cytochrome b-containing subunit HdrE. The HdrD subunit forms the catalytic center at the cytoplasmic side of the membrane (Fig. 9B) [33,34]. This reaction involves the two-electron reduction in CoM-S-S-CoB to the free thiols HS-CoB and HS-CoM [35]. Electrons are provided by reduced MPhen (MPhen_{red}), which are transferred via the heme groups of HdrE to the catalytic site of HdrD. This reaction is also coupled to a transfer of 2H⁺/2e⁻ (Fig. 8).

In addition to H₂, *M. thermophilum* can use formate as electron donor for the heterodisulfide reduction.



The key enzyme is a membrane-bound Fdh, which is well described in several bacteria. Formate dehydrogenase N from, for example, *E. coli* consists of the three subunits

FdnG, FdnH, and FdnI. FdnG forms the catalytic site containing FeS clusters and two molecules of molybdopterin-guanine dinucleotide (MGD) as prosthetic groups [25,36]. In some organisms, such as *Clostridium thermoaceticum* or *Campylobacter jejuni*, molybdate is replaced by tungstate [37,38]. The FdnH subunit coordinates four [4Fe-4S] clusters that mediate electron transfer from FdnG to FdnI. FdnI is a membrane-bound b-type cytochrome that transfers electrons to menaquinone [25,36]. In *M. thermophilum* homologues, subunits are present encoded in one cluster, and amino acids for binding of the prosthetic groups are conserved (Figs 8 and 9C). In some hydrogenotrophic methanogenic archaea, cytoplasmic forms of formate dehydrogenase were described, which transfer electrons to F₄₂₀ [39–42]. Other soluble formate dehydrogenases are coupled to the HdrABC complex and are involved in Fd_{red} formation [43–45]. Hence, cytoplasmic formate dehydrogenases play an important role in obligate hydrogenotrophic methanogens (reduction of F₄₂₀, Fd_{ox}, or CoM-S-S-CoB [13]), but none of these cytoplasmic enzymes is involved in respiratory electron transport.

The data presented here indicate that *M. thermophilum* possesses very similar electron transport systems and ion translocating enzymes (Fig. 8) as described for *M. mazei* (VhoGAC, HdrDE) and *E. coli* (FdnGHI): (a) DNA sequence analysis and amino acid sequence alignments revealed that all enzymes mentioned above show high similarities to the corresponding enzymes from *M. mazei*

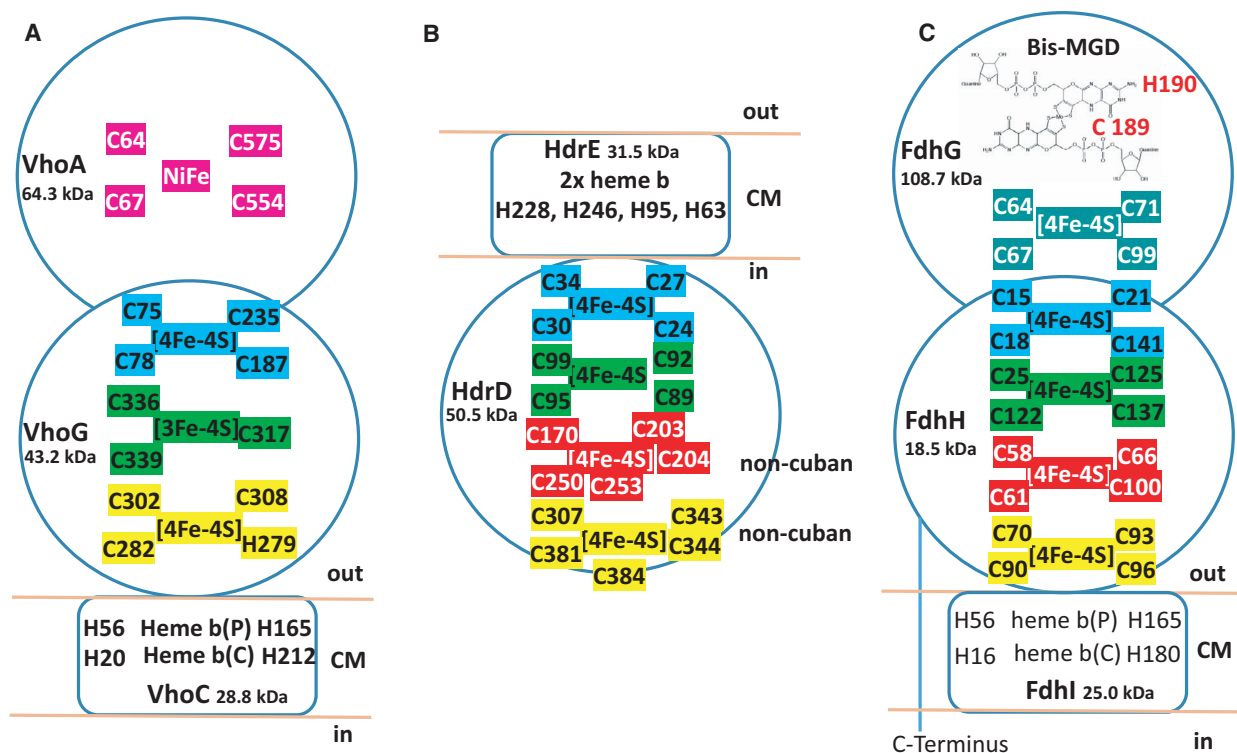


Fig. 9. Predicted structure and content of prosthetic groups in the respiratory complexes of *M. thermophilum*. (A) Vho hydrogenase, (B) heterodisulfide reductase, (C) formate dehydrogenase. The prediction of the overall structure and the coordinating amino acids is based on alignments with the corresponding enzymes from *E. coli* (FdnGHI, b1474–b1476), *Methanosarcina mazeri* (VhoGAC, AAM32008–AAM32010), and *Methanosarcina barkeri* (HdrDE, AKJ40005–AKJ40006). [4Fe-4S], 4 iron, 4 sulfur clusters; Bis-MGD, molybdopterin-guanine dinucleotide. The molybdate residue is coordinated by C189; NiFe, the catalytic nickel-iron cluster is covalently bound to the protein by the cysteine residues C64, C67, C575, and C554; noncubane [4Fe-4S], HdrD contains two unusual noncubane [4Fe-4S] clusters composed of fused [3Fe-4S][2Fe-2S] units sharing 1 iron and 1 sulfur. The heterodisulfide is clamped between the two noncubane [4Fe-4S] clusters and homolytically cleaved, forming HS-CoM and HS-CoB [35]; CM, cytoplasmic membrane.

and *E. coli*. Moreover, all amino acids are conserved, which are involved in the coordination of the essential prosthetic groups of VhoGAC, FdhGHI, and HdrDE (NiFe center, FeS clusters, heme groups, and MGD; Fig. 9). In addition, the signal peptide, which mediates the extracellular localization of VhoGA, is homologous. (b) In the presence of hydrogen and formate as electron donors and membranes of *M. thermophilum*, a reduction of about 390 and 190 nmol CoM-S-S-CoB $\text{min}^{-1}\cdot\text{mg protein}^{-1}$ could be observed, respectively. This value is comparable with respiratory electron transport activities in other methanogens such as *Methanosarcina mazeri*, *Methanobrevibacter smithii*, and *Methanomassiliococcus luminis* [28,46]. (c) The use of the water-soluble MPhen analogue OH-Phen allowed a more detailed analysis of the electron transport system in *M. thermophilum*. It was shown that OH-Phen is reduced by molecular hydrogen and formate as catalyzed by the Vho hydrogenase and Fdh formate dehydrogenase. Furthermore, the membrane-bound Hdr was able to use OH-Phen_{red} as

electron donor for the reduction in CoM-S-S-CoB. The results clearly indicated that a MPhen derivative could be present and could serve as an electron carrier in the membrane of *M. thermophilum*. (d) The membrane-bound electron transport systems (formate: heterodisulfide oxidoreductase and H_2 : heterodisulfide oxidoreductase) of *M. thermophilum* were inhibited by DPI. These effects are due to a complex interaction of DPI with the key enzymes of the electron transport chains. It was found that the reactions catalyzed by the Vho hydrogenase, formate dehydrogenase, and heterodisulfide reductase were inhibited by DPI. Interestingly, the H_2 -dependent and formate-dependent MV reduction as catalyzed by Vho and Fdh present in washed membranes was unaffected by DPI, respectively. This was also true for the heterodisulfide reduction by reduced methyl viologen as catalyzed by HdrDE. As DPI and phenazines are structurally similar with respect to their planar configuration, we assume that the inhibitor is able to bind to positions where interaction between phenazines (OH-Phen and

MPhen) and cytochrome b subunits of the key enzymes (VhoC, FdhI, HdrE) takes place (Figs 8 and 9) [28]. Since MV probably reacts directly with the FeS clusters of the catalytic subunits (VhoA, HdrD, and FdhG), electron transfer by DPI is not inhibited (Fig. 8). Again, these findings indicate that a phenazine derivate is the natural electron carrier responsible for electron transport from Vho/Fdh to Hdr. Our results are in line with the identification of a substance with a mass similar to MPhen in the membranes of *M. thermophilum* [7].

Electron transport is coupled to the formation of an electrochemical ion gradient, which can be used by an A_1A_o ATP synthase for ATP synthesis [12]. In general, protons and sodium ions can function as coupling ions. From the proposed reaction scheme shown in Fig. 8, it is obvious that VhoGAC and FdhGHI in *M. thermophilum* could translocate H^+ by scalar proton transfer. The same might be true for HdrDE. Mechanistically, it is difficult to assume that the enzymes transfer sodium ions across the membrane. Accordingly, we performed a sequence-based analysis of the ATP synthase subunit c in *M. thermophilum*, which defines the coupling ion specificity of the enzyme (not shown). In accordance with our hypothesis, the corresponding gene does not encode a typical sodium ion binding motif but only a glutamate residue that is sufficient for H^+ transport [47,48], indicating that an H^+ -dependent A_oA_1 -ATP synthase is present in *M. thermophilum*. As a consequence, adaptive strategies are needed for intracellular pH homeostasis. Not much is known about these processes in haloalkaliphilic methanogens but one strategy could be the expression of a Na^+/H^+ antiporter (OUJ19168.1-OUJ19176.1) that could contribute to ion homeostasis.

In summary, our experiments revealed that *M. thermophilum* possesses two variants of energy-conserving oxidoreductase systems in the membrane. These include the H_2 : heterodisulfide reductase system, which has already been described in *Methanosarcina* species, as well as the novel formate: heterodisulfide oxidoreductase system, which is unique for representatives of the class Methanonatronarchaea.

Materials and methods

Materials

All chemicals and reagents were obtained from Sigma-Aldrich (Munich, Germany) or Carl Roth (Karlsruhe, Germany).

Strains and culture conditions

Methanonatronarchaeum thermophilum AMET1 (DSM 28684) was obtained from the German Collection of

Microorganisms and Cell cultures (Braunschweig, Germany). Growth experiments were performed in a modified complex medium based on Hippe *et al.* [49] and Sorokin *et al.* [7]. The medium contains per liter: 0.35 g K_2HPO_4 , 0.23 g KH_2PO_4 , 0.5 g NH_4Cl , 0.5 g $MgSO_4 \times 7H_2O$, 0.25 g $CaCl_2 \times 2 H_2O$, 116.9 g NaCl, 2 mg $FeSO_4 \times 7 H_2O$, 1 mL trace element solution (DSMZ 1369) [50], 1 mL selenite tungstate solution (DSMZ_Medium 385), 1 mL trace element solution SL-6 (DSMZ_Medium 27), 2 g yeast extract, 2 g casein hydrolysate, 1 g Na acetate $\times 3 H_2O$, and 106 g Na_2CO_3 . The pH was adjusted to 9.5 with hydrochloric acid. Subsequently, the medium was filled in 50-mL or 500-mL serum flasks and gassed with N_2 for 10 min. Before closing, the flasks were gassed with a mix of N_2 (80%) and CO_2 (20%) for thirty seconds. After sterilization, 1 mL 10 x Wolin's vitamin solution (DSMZ Medium 141), 1 mL Hemin solution (DSMZ Medium 78), 250 μ L FeS suspension (DSMZ Medium 1267), and 100 μ M sodium 2-mercaptoethanesulfonate were added per liter. Subsequently, the methylated growth substrates were added in equal concentrations with respect to the number of methyl groups (33.3 mM TMA, 50 mM DMA, 100 mM MMA, 100 mM Methanol). 100 mM sodium formate was added for culture grown on formate. For growth with hydrogen, the serum flasks were gassed for one minute with 100% molecular hydrogen and an atmosphere of 200 kPa was adjusted. The gas phase was refreshed at regular intervals. Before inoculation, 1.5 mM cysteine and 0.5 mM sodium sulfide were added to the medium to remove residual oxygen. The cultures were incubated at 50 °C without agitation, and growth was observed by measuring the optical density (OD_{600}) at regular intervals.

Quantification of methane, methylamines, methanol, and formate

The CH_4 concentration was quantified by gas chromatography (GC). From the headspace of the culture, samples with a volume of 5–50 μ L were taken and injected into a gas chromatograph (PerkinElmer Clarus® 480, Rascon FFAP column 25 m \times 0.25 micron, PerkinElmer, Waltham, MA, USA) with a flame ionization detector (FID). Measurements were performed at a detector temperature of 250 °C, an injector temperature of 150 °C, and a column temperature of 120 °C with N_2 as carrier gas. Standards with a defined volume of methane were used as a reference.

TMA, DMA, and MMA consumption was analyzed in the medium. 500 μ L samples were taken, and cells were removed by centrifugation. Subsequently, 0.5% (v/v) H_2O_2 was added to the supernatant, and precipitates were removed by centrifugation. The further steps for the quantification of the three methylamines were performed as described by Krätzer *et al.* [21]. Methanol and formate were quantified via HPLC. The measurements were performed using an Aminex HPX-87H 300 mm \times 7.8 mm

column (Bio-Rad, Munich, Germany) with 5 mM H₂SO₄ as eluent at 65°C and a flow rate of 0.6 mL min⁻¹. For the preparation of samples, cells were removed by centrifugation from the medium and the supernatant was diluted in appropriate amounts with 5 mM H₂SO₄. Methanol and formate were quantified by standard curves.

Preparation of membrane fractions from *M. thermophilum*

The preparation of cytoplasmic membrane from *M. thermophilum* was performed anaerobically in an anaerobic chamber (Coy laboratory products, Grass Lake, Michigan, USA) under N₂ / H₂ atmosphere (98% / 2%, v/v). Five 1 L cultures of *M. thermophilum* were grown on methanol or TMA with formate or H₂ to the late exponential growth phase and were harvested by centrifugation (6000 g, 20 min, RT). The cell pellet was resuspended in a Tris/HCl buffer (100 mM Tris, 2 M NaCl, 5 mM dithiothreitol, 1 mg·L⁻¹ resazurin, pH 8.5), lysed by sonification, and centrifuged for 20 min at 11 000 g (4 °C) to remove the cell debris. The cell-free extract was ultracentrifuged at 150 000 g (2 h, 4 °C). The resulting supernatant was carefully removed, and the pellet was dissolved in the aforementioned Tris/HCl buffer. The ultracentrifugation step was repeated, the supernatant was discarded, and the membrane pellet was again homogenized in 1 mL Tris/HCl buffer. Membrane fractions were stored at -70 °C under a nitrogen atmosphere. The protein content was determined according to Bradford [51].

Enzyme reactions

All enzyme activities were analyzed at 50 °C. The determination of thiol formation from CoM-S-S-CoB by membranes of *M. thermophilum* in the presence of formate (10 mM) or molecular hydrogen was performed under an atmosphere of molecular hydrogen (H₂-dependent CoM-S-S-CoB reduction) or N₂ (formate-dependent CoM-S-S-CoB reduction) in 1-mL glass vials, filled with 200 µL 100 mM Tris/HCl buffer, pH 8.5 containing 2 M NaCl and 1 µg·mL⁻¹ resazurin. The buffer was reduced by titration with Ti(III)-citrate until resazurin turned colorless. After the addition of 50 µg membrane protein, the reaction was started with 5 mM CoM-S-S-CoB. To follow the reduction in CoM-S-S-CoB, aliquots of 5–20 µL were withdrawn and analyzed for thiol groups with Ellman's reagent as described [52]. DPI was solved in dimethyl sulfoxide and added as indicated in Fig. 6.

Enzymatic activities in washed membranes (1–5 µg protein) were measured in anaerobic cuvettes containing 700 µL buffer. For the analysis of H₂-dependent MV reduction, the assay was performed under an atmosphere of H₂, using a 100 mM Tris/HCl buffer pH 9.5 supplemented with 1 µg·mL⁻¹ resazurin, 2 M NaCl or 2 M KCl, and 5 mM

dithiothreitol. The reaction was started by the addition of 7 mM MV. Fdh activity was analyzed under an N₂ atmosphere using the same buffer. The final concentrations of the electron acceptor MV and electron donor formate were 7 mM and 10 mM, respectively. For measurement of HdrDE, a 100 mM Tris/HCl buffer, pH 8.5 containing 2 M KCl, 5 mM dithiothreitol, and 1 µg·mL⁻¹ resazurin were used. 7 mM MV was added and reduced by the addition of titanium citrate until an absorption of approximately 2.0 at 604 nm was reached. The reaction was started by the addition of membranes (1–5 µg protein) and 100 µM CoM-S-S-CoB. To determine the pH optima (Fig. 4A–C), a combined buffer system was used composed of Tris/HCl, MOPS, and glycine-HCl (50 mM final concentration each).

For measurements with OH-Phen, rubber-stoppered and N₂-flushed glass cuvettes were utilized, which were filled with 700 µL 100 mM Tris/HCl, pH 8.5, containing 2 M KCl, 5 mM dithiothreitol, 1 µg·mL⁻¹ resazurin, and 200 µM OH-Phen. Washed membranes of *M. thermophilum* (7.5 µg protein) were added to the assay, which was started by adding 50 µM formate or a stepwise addition of H₂. When the electron donors were oxidized, 1 mM heterodisulfide was added and the oxidation of OH-Phen_{red} was measured. Redox reactions with MV and OH-Phen were analyzed at 604 nm ($\epsilon_{MV} = 13.6 \text{ mM}^{-1}\cdot\text{cm}^{-1}$) and at 420 nm ($\epsilon_{OH-Phen} = 2.9 \text{ mM}^{-1}\cdot\text{cm}^{-1}$), respectively.

Bioinformatic analysis of the enzyme complexes involved in the energy metabolism of *M. thermophilum* AMET1 was performed by BLASTp analysis [53] and alignment analysis (Clustal Omega) [54].

Acknowledgements

The authors thank Natalie Thum-Schmitz (Institute of Microbiology and Biotechnology, University of Bonn, Germany) for technical assistance. UD was supported by the Deutsche Forschungsgemeinschaft (DE488/12-2), and DYS was supported by the Gravitation-SIAM Program of the Dutch Ministry of Education and Science (24002002).

Conflict of interest

There is no conflict of interest for all authors.

Author contributions

UD designed the study, wrote the paper, and analyzed data. FS planned and performed the experiments, wrote the paper, and contributed to the study's conception and to the data analysis. DYS supported the research and helped to cultivate *M. thermophilum*. All authors analyzed the results and approved the final version.

References

- Liu Y & Whitman WB (2008) Metabolic, phylogenetic, and ecological diversity of the methanogenic archaea. *Ann N Y Acad Sci* **1125**, 171–189.
- Bridgham SD, Cadillo-Quiroz H, Keller JK & Zhuang Q (2013) Methane emissions from wetlands: biogeochemical, microbial, and modeling perspectives from local to global scales. *Glob Chang Biol* **19**, 1325–1346.
- Mand TD & Metcalf WW (2019) Energy conservation and hydrogenase function in methanogenic archaea, in particular the genus *Methanosarcina*. *Microbiol Mol Biol Rev* **83**, e00020–e119.
- Ferry JG (2020) *Methanosarcina acetivorans*: A model for mechanistic understanding of acetate and reverse methanogenesis. *Front Microbiol* **11**, 1806.
- McGenity TJ (2010) In Methanogenesis and methanogenesis in hypersaline environments. In: Handbook of hydrocarbon and lipid microbiology (Timmis KN, McGenity TJ, van der Meer JR & de Lorenzo V, eds), pp. 665–680. Springer-Verlag, Berlin Heidelberg.
- Simankova MV, Kotsyurbenko OR, Lueders T, Nozhevnikova AN, Wagner B, Conrad R & Friedrich MW (2003) Isolation and characterization of new strains of methanogens from cold terrestrial habitats. *Syst Appl Microbiol* **26**, 312–318.
- Sorokin DY, Makarova KS, Abbas B, Ferrer M, Golyshin PN, Galinski EA & Koonin EV (2017) Discovery of extremely halophilic, methyl-reducing euryarchaea provides insights into the evolutionary origin of methanogenesis. *Nat Microbiol* **2**, 1–11.
- Sorokin DY, Merkel AY, Abbas B, Makarova KS, Rijpstra WIC, Koenen M, Sinnighe Damsté JS, Galinski EA, Koonin EV & van Loosdrecht MCM (2018) *Methanonatronarchaeum thermophilum* gen. nov., sp. nov. and '*Candidatus* Methanohalarchaeum thermophilum', extremely halo(natrono)philic methyl-reducing methanogens from hypersaline lakes comprising a new euryarchaeal class *Methanonatronarchaeia* classis nov. *Int J Syst Evol Microbiol* **68**, 2199–2208.
- Sorokin DY & Merkel AY (2019) Class *Methanonatronarchaeia*. In *Bergey's Manual of Systematics of Archaea and Bacteria* (Whitman WB, ed). John Wiley & Sons, Inc, Hoboken, NJ. <https://doi.org/10.1002/9781118960608.cbm00075>
- Sorokin DY & Merkel AY (2019) Genus *Methanonatronarchaeum*. In *Bergey's Manual of Systematics of Archaea and Bacteria* (Whitman WB, ed). John Wiley & Sons, Inc, Hoboken, NJ. <https://doi.org/10.1002/9781118960608.gbm01682>
- Costa KC & Leigh JA (2014) Metabolic versatility in methanogens. *Curr Opin Biotechnol* **29**, 70–75.
- Welte C & Deppenmeier U (2014) Bioenergetics and anaerobic respiratory chains of acetate-utilizing methanogens. *Biochim Biophys Acta* **1837**, 1130–1147.
- Yan Z & Ferry JG (2018) Electron bifurcation and confurcation in methanogenesis and reverse methanogenesis. *Front Microbiol* **9**, 1322.
- Deppenmeier U & Müller V (2008) Life close to the thermodynamic limit: how methanogenic archaea conserve energy. *Results Probl Cell Differ* **45**, 123–152.
- Kurth JM, Op den Camp HJM & Welte CU (2020) Several ways one goal-methanogenesis from unconventional substrates. *Appl Microbiol Biotechnol* **104**, 6839–6854.
- Müller V, Blaut M & Gottschalk G (1986) Utilization of methanol plus hydrogen by *Methanosarcina barkeri* for methanogenesis and growth. *Appl Environ Microbiol* **52**, 269–274.
- Fricke WF, Seedorf H, Henne A, Kruer M, Liesegang H, Hedderich R, Gottschalk G & Thauer RK (2006) The genome sequence of *Methanosphaera stadtmanae* reveals why this human intestinal archaeon is restricted to methanol and H₂ for methane formation and ATP synthesis. *J Bacteriol* **188**, 642–658.
- Dridi B, Fardeau ML, Ollivier B, Raoult D & Drancourt M (2012) *Methanomassiliococcus luminyensis* gen. nov., sp. nov., a methanogenic archaeon isolated from human faeces. *Int J Syst Evol Microbiol* **62**, 1902–1907.
- Kröniger L, Berger S, Welte C & Deppenmeier U (2016) Evidence for the involvement of two heterodisulfide reductases in the energy-conserving system of *Methanomassiliococcus luminyensis*. *FEBS J* **283**, 472–483.
- Kröniger L, Gottschling J & Deppenmeier U (2017) Growth characteristics of *Methanomassiliococcus luminyensis* and expression of methyltransferase encoding genes. *Archaea* **2017**, 2756573.
- Krätzer C, Carini P, Hovey R & Deppenmeier U (2009) Transcriptional profiling of methyltransferase genes during growth of *Methanosarcina mazei* on trimethylamine. *J Bacteriol* **191**, 5108–5115.
- Borrel G, Adam PS, McKay LJ, Chen LX, Sierra-García IN, Sieber CMK, Letourneur Q, Ghoulane A, Andersen GL, Li WJ *et al.* (2019) Wide diversity of methane and short-chain alkane metabolisms in uncultured archaea. *Nat Microbiol* **4**, 603–613.
- Wu LF, Chanal A & Rodrigue A (2000) Membrane targeting and translocation of bacterial hydrogenases. *Arch Microbiol* **173**, 319–324.
- Eismann K, Mlejnek K, Zipprich D, Hoppert M, Gerberding H & Mayer F (1995) Antigenic determinants of the membrane-bound hydrogenase in *Alcaligenes eutrophus* are exposed toward the periplasm. *J Bacteriol* **177**, 6309–6312.
- Jormakka M, Törnroth S, Byrne B & Iwata S (2002) Molecular basis of proton motive force generation:

- structure of formate dehydrogenase-N. *Science* **295**, 1863–1868.
- 26 Ragan CI (1976) NADH-ubiquinone oxidoreductase. *Biochim Biophys Acta* **456**, 249–290.
- 27 Majander A, Finel M & Wikstrom M (1994) Diphenyleneiodonium inhibits reduction of iron-sulfur clusters in the mitochondrial NADH ubiquinone oxidoreductase. *J Biol Chem* **269**, 21037–21042.
- 28 Brodersen J, Bäumer S, Abken HJ, Gottschalk G & Deppenmeier U (1999) Inhibition of membrane-bound electron transport of the methanogenic archaeon *Methanosarcina mazei* Gö1 by diphenyleneiodonium. *Eur J Biochem* **259**, 218–224.
- 29 Thauer RK, Kaster AK, Seedorf H, Buckel W & Hedderich R (2008) Methanogenic archaea: ecologically relevant differences in energy conservation. *Nat Rev Microbiol* **6**, 579–591.
- 30 Kaster AK, Moll J, Parey K & Thauer RK (2011) Coupling of ferredoxin and heterodisulfide reduction via electron bifurcation in hydrogenotrophic methanogenic archaea. *Proc Natl Acad Sci USA* **108**, 2981–2986.
- 31 Kulkarni G, Mand TD & Metcalf WW (2018) Energy conservation via hydrogen cycling in the methanogenic archaeon *methanosarcina barkeri*. *mBio* **9**, e01256–e1318.
- 32 Dubini A & Sargent F (2003) Assembly of Tat-dependent [NiFe] hydrogenases: identification of precursor-binding accessory proteins. *FEBS Lett* **549**, 141–146.
- 33 Hedderich R, Hamann N & Bennati M (2005) Heterodisulfide reductase from methanogenic archaea: a new catalytic role for an iron-sulfur cluster. *Biol Chem* **386**, 961–970.
- 34 Simianu M, Murakami E, Brewer JM & Ragsdale SW (1998) Purification and properties of the heme- and iron-sulfur-containing heterodisulfide reductase from *Methanosarcina thermophila*. *Biochemistry* **37**, 10027–10039.
- 35 Wagner T, Koch J, Ermler U & Shima S (2017) Methanogenic heterodisulfide reductase (HdrABC-MvhAGD) uses two noncubane [4Fe-4S] clusters for reduction. *Science* **357**, 699–703.
- 36 Jormakka M, Byrne B & Iwata S (2003) Formate dehydrogenase—a versatile enzyme in changing environments. *Curr Opin Struct Biol* **13**, 418–423.
- 37 Ljungdahl LG & Andreessen JR (1975) Tungsten, a component of active formate dehydrogenase from *Clostridium thermoacetum*. *FEBS Lett* **54**, 279–282.
- 38 Smart JP, Cliff MJ & Kelly DJ (2009) A role for tungsten in the biology of *Campylobacter jejuni*: tungstate stimulates formate dehydrogenase activity and is transported via an ultra-high affinity ABC system distinct from the molybdate transporter. *Mol Microbiol* **74**, 742–757.
- 39 Ferry JG (1990) Formate dehydrogenase. *FEMS Microbiol Rev* **7**, 377–382.
- 40 Schauer NL & Ferry JG (1986) Composition of the coenzyme F₄₂₀-dependent formate dehydrogenase from *Methanobacterium formicicum*. *J Bacteriol* **165**, 405–411.
- 41 Baron SF & Ferry JG (1989) Reconstitution and properties of a coenzyme F₄₂₀-mediated formate hydrogenlyase system in *Methanobacterium formicicum*. *J Bacteriol* **171**, 3854–3859.
- 42 Sattler C, Wolf S, Fersch J, Goetz S & Rother M (2013) Random mutagenesis identifies factors involved in formate-dependent growth of the methanogenic archaeon *Methanococcus maripaludis*. *Mol Genet Genomics* **288**, 413–424.
- 43 Abdul Halim MF, Day LA & Costa KC (2021) Formate-dependent heterodisulfide reduction in a Methanomicrobiales Archaeon. *Appl Environ Microbiol* **87**, e02698–e2720.
- 44 Milton RD, Ruth JC, Deutzmann JS & Spormann AM (2018) *Methanococcus maripaludis* employs three functional heterodisulfide reductase complexes for flavin-based electron bifurcation using hydrogen and formate. *Biochemistry* **57**, 4848–4857.
- 45 Costa KC, Wong PM, Wang T, Lie TJ, Dodsworth JA, Swanson I, Burn JA, Hackett M & Leigh JA (2010) Protein complexing in a methanogen suggests electron bifurcation and electron delivery from formate to heterodisulfide reductase. *Proc Natl Acad Sci USA* **107**, 11050–11055.
- 46 Kröninger L, Steiniger F, Berger S, Kraus S, Welte CU & Deppenmeier U (2019) Energy conservation in the gut microbe *Methanomassiliococcus luminyensis* is based on membrane-bound ferredoxin oxidation coupled to heterodisulfide reduction. *FEBS J* **286**, 3831–3843.
- 47 Rahlfs S & Müller V (1997) Sequence of subunit c of the Na⁺-translocating F₁F₀ ATPase of *Acetobacterium woodii*: proposal for determinants of Na⁺ specificity as revealed by sequence comparisons. *FEBS Lett* **404**, 269–271.
- 48 Grüber G, Manimekalai MS, Mayer F & Müller V (2014) ATP synthases from archaea: the beauty of a molecular motor. *Biochim Biophys Acta* **1837**, 940–952.
- 49 Hippe H, Caspari D, Fiebig K & Gottschalk G (1979) Utilization of trimethylamine and other N-methyl compounds for growth and methane formation by *Methanosarcina barkeri*. *Proc Natl Acad Sci USA* **76**, 494–498.
- 50 Pfennig N & Lippert KD (1966) Über das Vitamin B₁₂-Bedürfnis phototropher Schwefelbakterien. *Arch Mikrobiol* **55**, 245–256.
- 51 Bradford MM (1976) A rapid and sensitive method for the quantitation of microgram quantities of protein utilizing the principle of protein-dye binding. *Anal Biochem* **72**, 248–254.

- 52 Ellman GL (1959) Tissue sulfhydryl groups. *Arch Biochem Biophys* **82**, 70–77.
- 53 Altschul SF, Gish W, Miller W, Myers EW & Lipman DJ (1990) Basic local alignment search tool. *J Mol Biol* **215**, 403–410.
- 54 Madeira F, Park YM, Lee J, Buso N, Gur T, Madhusoodanan N, Basutkar P, Tivey ARN, Potter SC, Finn RD *et al.* (2019) The EMBL-EBI search and sequence analysis tools APIs in 2019. *Nucleic Acids Res* **47** (W1), W636–W641.